Joint Special Interest Group meeting between euspen and ASPE
Advancing Precision in Additive Manufacturing
TU Berlin, Germany, October 2025
www.euspen.eu

Powder spreading characterization in additive manufacturing using the NIST powder spreading test bed (PST)

Jesse Redford[1], Aniruddha Das[1], Eric Whitenton[1]

[1] *National Institute of Standards and Technology (NIST), Gaithersburg, MD, USA*

Abstract

The success of powder bed fusion additive manufacturing (PBF-AM) hinges on the ability to consistently spread thin, even layers of powder for subsequent fusion. The powder spreading test bed (PST) aims to provide new insights into the powder spreading in PBF-AM by capturing the first-ever cross-sectional high-speed images of the entire process. Procedures were developed to control key spreading parameters, including the powder dosage, recoating gap, and blade speed, mimicking conditions that occur in commercial machines. The recent upgrades are enabling the development and validation of spreadability metrics for AM feedstock materials and PBF-AM processes. A high-level summary of recent improvements made to the PST, data collection efforts, and plans for future investigations are provided.

Powder spreading, powder spreadability, particle image velocimetry, characterization, powder bed fusion, additive manufacturing.

1. Introduction

Metal powder spreading for additive manufacturing has been studied widely with various spreading testbeds and other apparatuses [1–4]. However, only a small number of custom-built powder spreading testbeds have enabled cross-sectional imaging of the powder during spreading, and among these, only two have demonstrated sufficient spatial and temporal resolution to support particle image velocimetry (PIV) analysis of internal flow fields [3–5]. However, both platforms employ stationary high-speed cameras fixed in the laboratory frame, which substantially limits the observation window of the spreading process. Specifically, the camera field of view captures the region in front of the recoater blade for only a brief duration as it passes by, typically less than 300 ms, resulting in incomplete temporal coverage of the spreading process. This restricted observation interval constrains the ability to resolve transient or spatially localized powder behavior during spreading. The National Institute of Standards and Technology (NIST) powder spreading test bed (PST) has been updated with an imaging configuration in which the camera can translate synchronously with the recoater blade. This moving-frame-of-reference approach enables continuous visualization of the powder throughout the entire spreading sequence, capturing its formation, spreading, and eventual depletion, providing complete temporal coverage compared to a static imaging configuration. Metrics extracted from image analysis and PIV can be more easily compared and statistically averaged over larger temporal durations, enabling the identification of both transient and quasi-steady-state behaviors, such as intermittent particle jamming that may be completely missed in a stationary camera setup.

2. Methodology

An example of the NIST PST with the moving camera configuration is shown in Figure 1. Both ceramic and highspeed steel (HSS) recoater blades used in commercial machines can be installed on the recoater arm. A highspeed camera is fixed to a secondary stage and can be programmed to move in parallel with the recoater arm. Offsets can be prescribed to position the blade anywhere within the field of view (FOV) of the camera. The high-speed camera can currently be configured with the different telecentric lenses listed in Table 1. The PST allows for spreading velocities up to 250 mm/s, well above the default speed for most commercial PBF-LB machines, typically ranging between 50 mm/s and 150 mm/s [1, 6, 7].

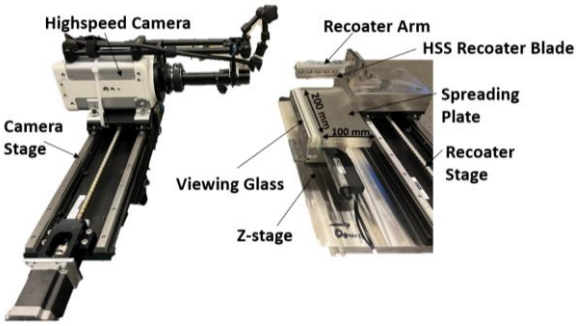

Figure 1. Example of NIST powder spreading test bed configured in moving camera arrangement for continuous cross-sectional imaging of the entire powder spreading process.

Table 1 Summary of lens configurations and corresponding field of view and spatial resolution for high-speed cross-sectional imaging.

Telecentric Lens	Extender	Field of view N x N (mm)	Spatial Resolution (µm/pixel)
4 X	1 X	3.89 × 3.89	3.81
	1.4 X	2.77 × 2.77	2.71
	2 X	1.93 × 1.93	1.89
6 X	1 X	2.59 × 2.59	2.54
	1.4 X	1.85 × 1.85	1.81
	2 X	1.28 × 1.28	1.26

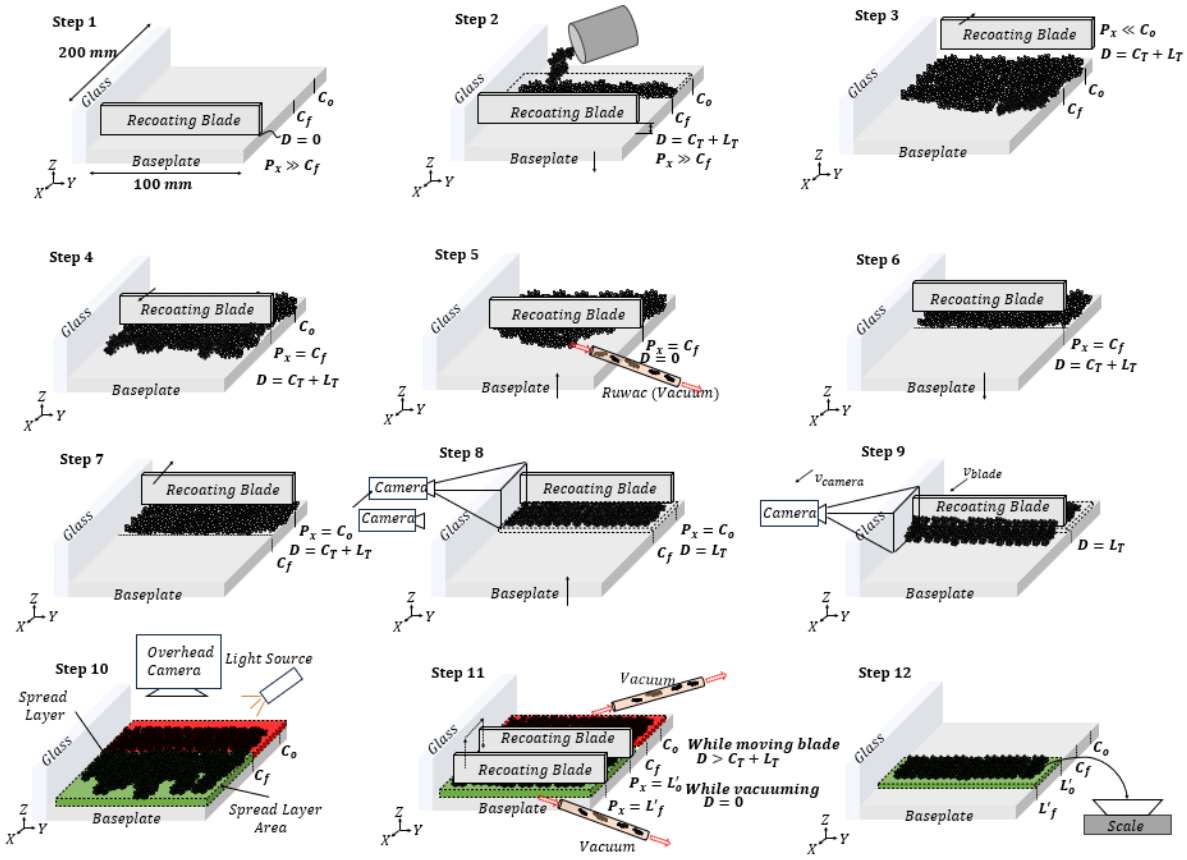

Figure 2. Example of steps involved in creating a well-controlled volume of powder for spreading experiments and isolation of a portion of the spread layer for subsequent layer density measurements. Commanded positions of the recoater arm are given by P_x. The recoater gap D is the distance between blade edge and the baseplate controlled by the Z-stage. L_T is the programmed powder layer thickness. C_T represents the thickness of the initial powder charge used for spreading and the difference between positions C_f and C_o represent the charge length.

The first objective of upgrading the testbed was to create a repeatable powder dispensing method, such that given the same spreading conditions, when the blade reaches a fixed position along the baseplate during the spreading process, the size of the imaged powder heap (i.e., powder in front of the recoater blade) is consistent across multiple repeat experiments. To achieve this, steps 1-8 in the procedures shown in Figure 2 were developed to precisely control the creation of the initial powder dosage for spreading a layer, mimicking the spreading conditions of a commercial machine with a dispensing mechanism. However, for the PST, no dispensing stage is used to avoid powder leakage through the interface between the baseplate and the dispensing stage. Leakage or loss of powder affected the heap size, rendering non-repeatable observations. Without consistent observations under the same spreading conditions, isolating the direct impact of spreading parameters and changes in powder morphology, size, and other characteristics cannot be isolated to explain spreadability. The actual spreading and data acquisition process begins at step 9, where both the camera and recoater stages move together at the same velocity such that cross-sectional imaging of the entire spreading process is obtained. The areas highlighted in green in step 10 represent the spread layer area. Notice that the layer starts where the charge area C_f ends and terminates at whatever position the recoater reaches when the powder is fully depleted (e.g., no powder remains in front of the blade). After spreading, an overhead camera is used to capture a top-down image of the spread layer under different lighting conditions. In step 11, the recoater blade is programmed to move to defined conditions and provide a barrier such that powder outside of a designated fixed region can be vacuumed away. The remaining area shown in step 12 provides a way to sample the powder within a well-known volume governed by the width of the base plate, programmed positions, and initial programmed recoater gap (D) within the spread layer area. The mass can be weighed and divided by this theoretical volume to obtain measurements of the spread layer density. Figure 3 provides a cross-sectional view of step 8 prior to spreading initiation. The center image represents the point at which the spreading of the layer begins, as at this point the powder in front of the heap begins to deplete under the blade.

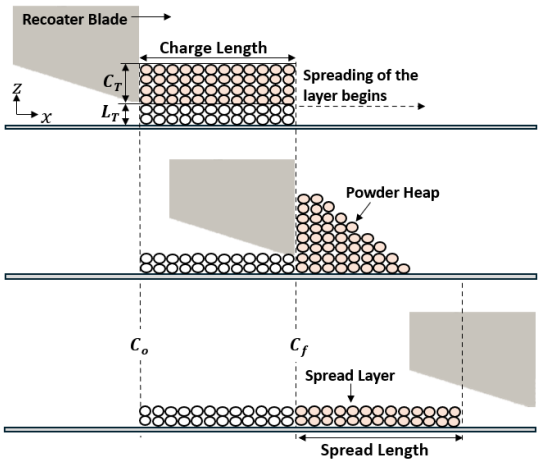

Figure 3. Example of preparation and control over the initial charge of powder and the layer thickness for spreading experiments.

Table 2 provides an overview of the controllable spreading conditions and various forms of data collection that will be included in future studies and public datasets.

Table 2 High level summary of controllable spreading conditions and examples of the types of data that will be collected for powder characterization.

Spreading Conditions	Data Collection		
	During Spreading	After Spreading	Auxiliary
Powder Type	High-speed cross-sectional imaging of the powder and metrics derived from this data	Profile or Areal Topography	SEM Images & Morphology Metrics
Recoater Blade	Particle tracking data & PIV	Overhead image of the spread layer under different light conditions	Powder Size Distribution
Charge Thickness	Dynamic angle of repose	Isolated spread layer density	Rotating Drum Metrics
Charge Length	Heap area in front of the blade and the mean and standard deviation of the first time derivate of this quantity		Hall Flow and Hall Density
Recoater Gap			Static angle of repose
Recoater Speed			

The PST enables modifications to the spreading conditions, including the dosage of powder governed by the charge thickness and length, as well as deposition settings controlled by the recoating gap, velocity, and blade geometry. Detailed alignment routines have been developed to facilitate relocation of the entire setup as needed. Data collection during powder spreading consists of high-speed cross-sectional imaging of the entire spreading process. From this video data, automated image processing routines are being developed to measure the time-dependent cross-sectional area of the powder in front of the blade $A_{heap}(t)$, the average and standard deviation of the first-time derivative of this quantity (e.g., depletion rate $\frac{dA_{heap}}{dt}$) and the dynamic avalanche angle $\theta_{heap}(t)$. Particle image velocimetry (PIV) is also being used to track particle trajectories and generate spatially resolved velocity maps, providing insights into aggregate and individual particle flow behavior during spreading. Data collected after spreading includes overhead images of the spread layer under different lighting conditions, providing insight into the homogeneity and coverage of the spread layer enabling additional evaluations of spread quality. Measurement of the spread layer density is also being used to investigate the cause-and-effect relationship between changes in process parameters (e.g., recoater gap, recoating velocity, particle size distribution) and the spreadability of the powder. Future modifications to the PST's recoater may include the addition of overhead apparatuses for measuring the surface topography of the spread powder layer. Auxiliary data includes additional metrics obtained through various test methods, such as the powder size distribution and scanning electron microscope (SEM) images to characterize powder morphology. The current data collection list in Table 2 is not exhaustive, but it represents the types of data that will be collected for the release of an initial dataset.

2.1 *Automation of measurements during powder spreading*

To remove operator subjectivity, the avalanche angle (i.e., dynamic angle of repose) of the powder heap is computed automatically for each video frame using a binary mask $I_{binary}(x, y)$ obtained via adaptive thresholding and morphological filtering. For each column x_i where heap material is detected, the topmost foreground pixel is extracted as $y_i = min\{y \mid I_{binary}(x_i, y) = 1\}$. The resulting set of (x_i, y_i) coordinates define the free surface of the powder heap in front of the blade. A first-order polynomial $y = ax + b$ is fitted to this edge using ordinary least squares, and the avalanche angle θ_{heap} is defined as $\theta_{heap} = arctan\,(a)$, with θ_{heap} expressed in degrees. This angle provides a time-resolved, quantitative measure of the heap's dynamic front-face inclination during the spreading process. Frames where the coefficient of determination R^2 of the fitted line is less than 0.95 are currently excluded from statistics as shown in the bottom image of Figure 4. Figure 4 shows representative frames of the automatically generated contour enclosing the powder in front the recoater and fitted heap profile (white line) used to determine θ_{heap} overlaid.

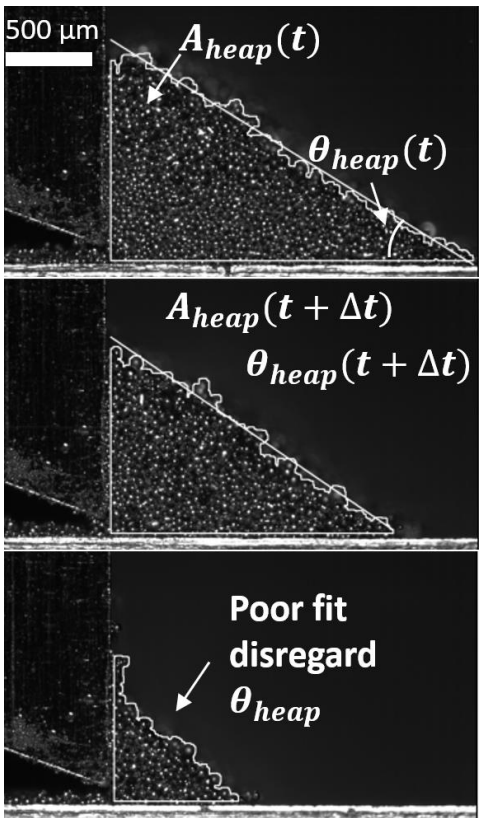

Figure 4. Example of automated segmentation of the powder in front of the recoater blade at different times during the spreading process.

Ongoing efforts are focused on streamlining both data collection and data organization processes to enable the generation of a complete dataset immediately after the experiment. This includes automating and reducing the computation time of the particle image velocimetry (PIV) workflow originally developed in [5] for the static camera setup.

3. Discussion

The development of a comprehensive dataset to better understand powder spreading in additive manufacturing requires a thorough evaluation of measurement uncertainty. To achieve this, both Type A and Type B uncertainty evaluations are being developed for each measurand derived from the data. Repeat experiments with identical powders and spreading conditions are being performed over extended periods to assess the repeatability and reproducibility of the established and developing measurements. This information is crucial for determining the sensitivity of different metrics in distinguishing between changes driven by altered spread parameters and/or feedstock characteristics and those resulting from measurement uncertainty. Preliminary findings indicate that the relative Type A uncertainty for the spread layer density measurements can be less than 1 % between repeat experiments, demonstrating the testbed's capability to support rigorous metrological studies. The low variability within identical conditions reinforces the reliability of the spreading and measurement process. Furthermore, the metrics obtained from the PST are being compared to both emerging and standardized test methods to establish fundamental relationships between bulk metal powder characteristics and powder spreading performance. Ongoing research will continue to elucidate these relationships and complex interactions governing powder spreading, with findings to be reported in the presentation and future publications.

4. Conclusions and future work

This work has provided a high-level overview of the PST's operating procedures and developing data collection strategies. The NIST PST is being further improved to provide a comprehensive understanding of powder spreading in additive manufacturing. By bridging the gap between common powder characterization methods and measurements directly linked to spreadability, the PST will support the development of predictive frameworks that relate powder properties and spreading conditions to layer quality. The insights generated from the PST are expected to inform future standards development and improve powder qualification protocols and test methods across the AM supply chain.

NIST Disclaimer

 The full descriptions of the procedures used in this paper require the identification of certain commercial products. The inclusion of such information should in no way be construed as indicating that such products are endorsed by NIST or are recommended by NIST or that they are necessarily the best materials, instruments, software, or suppliers for the purposes described.

References

[1] Oropeza D, Roberts R, Hart AJ (2021) A modular testbed for mechanized spreading of powder layers for additive manufacturing. *Review of Scientific Instruments* **92**(1):015114. https://doi.org/10.1063/5.0031191

[2] Brika SE, Brailovski V (2023) A Novel Apparatus for the Simulation of Powder Spreading Procedures in Powder-Bed-Based Additive Manufacturing Processes: Design, Calibration, and Case Study. *Journal of Manufacturing and Materials Processing* **7**(4):135. https://doi.org/10.3390/jmmp7040135

[3] Whiting J, Whitenton E, Das A, Tondare V, Fox J, McGlauflin M, Donmez A, Moylan SP (2023) Powder Spreading Testbed for Studying the Powder Spreading Process in Powder Bed Fusion Machines. *NIST Advanced Manufacturing Series* **100**(56). https://doi.org/10.6028/NIST.AMS.100-56

[4] Yim S, Sun J, Minowa K, Wang H, Aoyagi K, Yamanaka K, Chiba A (2023) In-situ observation of powder spreading in powder bed fusion metal additive manufacturing process using particle image velocimetry. *Additive Manufacturing* **78**:103823. https://doi.org/10.1016/j.addma.2023.103823

[5] Eric Whitenton, Justin Whiting, Alkan Donmez, Aniruddha Das, Vipin Tondare, Jason Fox, Michael McGlaufin, Shawn Moylan (2023) Implementation of a Particle Tracking Method to Study Particle Spreading in Powder Bed Fusion Systems. *NIST Advanced Manufacturing Series* **100**(58). https://doi.org/10.6028/NIST.AMS.100-58

[6] Snow Z, Martukanitz R, Joshi S (2019) On the development of powder spreadability metrics and feedstock requirements for powder bed fusion additive manufacturing. *Additive Manufacturing* **28**:78–86. https://doi.org/10.1016/j.addma.2019.04.017

[7] Horn M, Schmitt M, Langer L, Schlick G, Seidel C (2024) Laser powder bed fusion recoater selection guide—Comparison of resulting powder bed properties and part quality. *Powder Technology* **434**:119356. https://doi.org/10.1016/j.powtec.2023.119356